

Synchronization of weakly coupled oscillators: coupling, delay and topology

This content has been downloaded from IOPscience. Please scroll down to see the full text.

2013 J. Phys. A: Math. Theor. 46 505101

(<http://iopscience.iop.org/1751-8121/46/50/505101>)

View [the table of contents for this issue](#), or go to the [journal homepage](#) for more

Download details:

IP Address: 128.84.94.80

This content was downloaded on 06/12/2013 at 20:19

Please note that [terms and conditions apply](#).

Synchronization of weakly coupled oscillators: coupling, delay and topology

Enrique Mallada and Ao Tang

School of ECE, Cornell University, Ithaca, NY 14853, USA

E-mail: em464@cornell.edu and atang@ece.cornell.edu

Received 13 July 2013, in final form 2 October 2013

Published 26 November 2013

Online at stacks.iop.org/JPhysA/46/505101

Abstract

There are three key factors in a system of coupled oscillators that characterize the interaction between them: *coupling* (*how to affect*), *delay* (*when to affect*) and *topology* (*whom to affect*). The existing work on each of these factors has mainly focused on special cases. With new angles and tools, this paper makes progress in relaxing some assumptions on these factors. There are three main results in this paper. Firstly, by using results from algebraic graph theory, a sufficient condition is obtained that can be used to check equilibrium stability. This condition works for arbitrary topology, generalizing existing results and also leading to a sufficient condition on the coupling function which guarantees that the system will reach synchronization. Secondly, it is known that identical oscillators with $\sin()$ coupling functions are guaranteed to synchronize in phase on a complete graph. Our results prove that in many cases certain structures such as symmetry and concavity, rather than the exact shape of the coupling function, are the keys for global synchronization. Finally, the effect of heterogeneous delays is investigated. Using mean field theory, a system of delayed coupled oscillators is approximated by a non-delayed one whose coupling depends on the delay distribution. This shows how the stability properties of the system depend on the delay distribution and allows us to predict its behavior. In particular, we show that for $\sin()$ coupling, heterogeneous delays are equivalent to homogeneous delays. Furthermore, we can use our novel sufficient instability condition to show that heterogeneity, i.e. wider delay distribution, can help reach in-phase synchronization.

PACS number: 05.45.Xt

(Some figures may appear in colour only in the online journal)

1. Introduction

Systems of coupled oscillators have been widely studied in different disciplines ranging from biology [1–5] and chemistry [6, 7] to engineering [8, 9] and physics [10, 11]. The possible behavior of such systems can be complex. For example, the intrinsic symmetry of the network can produce multiple limit cycles or equilibria with relatively fixed phases (phase-locked trajectories) [12], which in many cases can be stable [13]. Also, the heterogeneity in the natural oscillation frequency can lead to incoherence [14] or even chaos [15].

A particularly interesting question is whether the coupled oscillators will synchronize in phase in the long run [16–20]. Besides its clear theoretical value, it also has rich applications in practice.

In essence, there are three key factors in a system of coupled oscillators that characterize the interaction between oscillators: *coupling*, *delay* and *topology*. For each of these, the existing work has mainly focused on special cases as explained below. In this paper, further research will be discussed on each of the three factors.

- *Topology (whom to affect, section 3.2)*. Current results either restrict to complete graph or a ring topology for analytical tractability [19], study *local stability* of topology independent solutions over time-varying graph [21–23], or introduce dynamic controllers to achieve synchronization for time-varying uniformly connected graphs [24, 25]. We develop a graph-based sufficient condition which can be used to check equilibrium instability for any fixed topology. It also leads to a family of coupling functions guaranteeing that the system will reach *global* phase consensus for arbitrary connected undirected graphs using only physically meaningful state variables.
- *Coupling (how to affect, section 3.3)*. The classical Kuramoto model [14] assumes a $\sin(\cdot)$ coupling function. Our study suggests that certain symmetry and convexity structures suffice to guarantee global synchronization. We show that most orbits that appear due to symmetries on a complete graph are unstable provided that the coupling function is even and concave on $[0, \pi]$ and its derivative is concave on $[-\frac{\pi}{2}, \frac{\pi}{2}]$.
- *Delay (when to affect, section 4)*. Existing work generally assumes zero delay among oscillators or requires them to be bounded up to a constant fraction of the period [26]. This is clearly unsatisfactory especially if the oscillating frequencies are high. We use mean field theory to study unbounded delays by constructing a non-delayed phase model that is equivalent to the original one in the large population limit. Using this novel technique, we then show that when the system has $\sin(\cdot)$ coupling, heterogeneous delays and homogeneous delays are equivalent. Finally, we use our novel graph-based instability condition to illustrate how a slight increase in the heterogeneity of the delays can make certain non-in-phase equilibria unstable and therefore promote in-phase synchronization.

This paper focuses on *weakly* coupled oscillators, which can be either pulse-coupled or phase-coupled. Although most of the results presented are for phase-coupled oscillators, they can be readily extended for pulse-coupled oscillators (see, e.g., [27, 28]). It should be noted that results in section 3 are independent of the strength of the coupling and therefore do not require inclusion of the weak coupling assumption. Preliminary versions of this work have been presented in [29, 30].

The paper is organized as follows. We describe pulse-coupled and phase-coupled oscillator models, as well as their common weak coupling approximation, in section 2. Using some facts from algebraic graph theory and potential dynamics in section 3.1, we present the negative cut instability theorem in section 3.2.1 to check whether an equilibrium is unstable. This leads to theorem 1 in section 3.2.2 which identifies a class of coupling functions that guarantee that

the system always synchronizes in phase. It is well known that the Kuramoto model produces global synchronization over a complete graph. In section 3.3, we demonstrate that a large class of coupling functions, in which the Kuramoto model is a special case, guarantee the instability of most of the limit cycles in a complete graph network. Section 4 is devoted to the discussion of the effect of delay. An equivalent non-delayed phase model is constructed whose coupling function is the convolution of the original coupling function and the delay distribution. Using this approach, we show that for the Kuramoto model (with homogeneous frequencies), heterogeneous delays and homogeneous delays are equivalent (section 4.1). Finally, we show in section 4.2 that sometimes more heterogeneous delays among oscillators can help reach synchronization. Our conclusions are presented in section 5.

2. Coupled oscillators

We consider two different models of coupled oscillators analyzed in the literature. The difference between the models arises in the interactions between the oscillators, and their dynamics can be quite different. However, when the interactions are weak (weak coupling), both systems behave similarly and share the same approximation. This allows us to study them under a common framework.

Each oscillator is represented by a phase θ_i in the unit circle \mathbb{S}^1 which in the absence of coupling moves with constant speed $\dot{\theta}_i = \omega$. Here, \mathbb{S}^1 represents the unit circle, or equivalently the interval $[0, 2\pi]$ with 0 and 2π identified ($0 \equiv 2\pi$), and $\omega = \frac{2\pi}{T}$ denotes the natural frequency of the oscillation.

2.1. Pulse-coupled oscillators

In this model the interaction between oscillators is performed by pulses. An oscillator j sends out a pulse whenever it crosses zero ($\theta_j = 0$). When oscillator i receives a pulse, it will change its position from θ_i to $\theta_i + \varepsilon \kappa_{ij}(\theta_i)$. The function κ_{ij} represents how other oscillator actions affect oscillator i and the scalar $\varepsilon > 0$ is a measure of the coupling strength. These jumps can be modeled by a Dirac delta function δ satisfying $\delta(t) = 0 \forall t \neq 0$, $\delta(0) = +\infty$, and $\int \delta(s) ds = 1$. The coupled dynamics are represented by

$$\dot{\theta}_i(t) = \omega + \varepsilon \omega \sum_{j \in \mathcal{N}_i} \kappa_{ij}(\theta_i(t)) \delta(\theta_j(t - \eta_{ij})), \quad (1)$$

where $\eta_{ij} > 0$ is the propagation delay between oscillators i and j ($\eta_{ij} = \eta_{ji}$), and \mathcal{N}_i is the set of i 's neighbors. The factor of ω in the sum is needed to keep the size of the jump within $\varepsilon \kappa_{ij}(\theta_i)$. This is because $\theta_j(t)$ behaves like ωt when crosses zero and therefore the jump produced by $\delta(\theta_j(t))$ is of size $\int \delta(\theta_j(t)) dt = \omega^{-1}$ [28].

The coupling function κ_{ij} can be classified based on the qualitative effect it produces in the absence of delay. After one period, if the net effect of the mutual jumps brings a pair of oscillators closer, we call it **attractive** coupling. If the oscillators are brought further apart, it is considered to be **repulsive** coupling. The former can be achieved, for instance, if $\kappa_{ij}(\theta) \leq 0$ for $\theta \in [0, \pi)$ and $\kappa_{ij}(\theta) \geq 0$ for $\theta \in [\pi, 2\pi)$. See figure 1 for an illustration of an attractive coupling κ_{ij} and its effect on the relative phases.

This pulse-like interaction between oscillators was first introduced by Peskin [2] in 1975 as a model of the pacemaker cells of the heart, although the canonic form did not appear in the literature until 1999 [28]. In general, when the number of oscillators is large, there are several different limit cycles besides the in-phase synchronization and many of them can be stable [13].

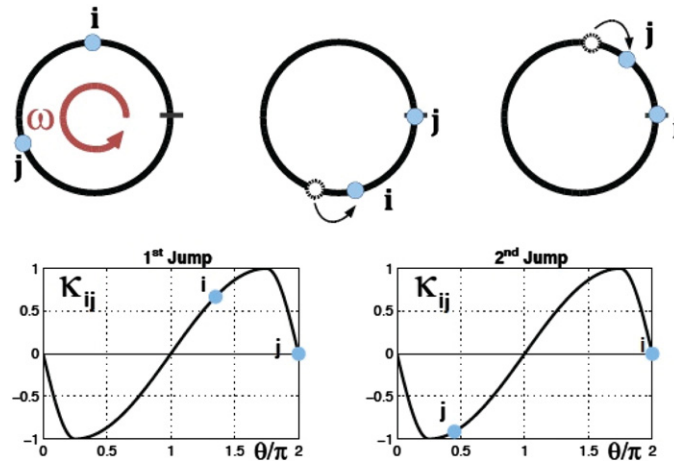


Figure 1. Pulse-coupled oscillators with attractive coupling. The jumps of oscillators i and j are illustrated at the top. The bottom charts show the value of the coupling function at the instants when either j or i send a pulse. After one cycle, both oscillators end up closer (attractive coupling).

The question of whether this system can collectively achieve in-phase synchronization was answered for the complete graph case and zero delay by Mirollo and Strogatz in 1990 [20]. They showed that if $\kappa_{ij}(\theta)$ is strictly increasing on $(0, 2\pi)$ with a discontinuity in 0 (which resembles attractive coupling), then for almost every initial condition, the system can synchronize in phase in the long run.

The two main assumptions of [20] are all to all communication and zero delay. Whether in-phase synchronization can be achieved for arbitrary graphs has been an open problem for over twenty years. On the other hand, when delay among oscillators is introduced the analysis becomes intractable. Even in the case of two oscillators, there is a large number of possibilities to be considered [31, 32].

2.2. Phase-coupled oscillators

In the model of phase-coupled oscillators, the interaction between neighboring oscillators i and $j \in \mathcal{N}_i$ is modeled by change of the oscillating speeds. Although the speed change can generally be a function of both phases (θ_i, θ_j) , we concentrate on the case where the speed change is a function of the phase differences $f_{ij}(\phi_j(t - \eta_{ij}) - \phi_i(t))$. Thus, since the net speed change of oscillator i amounts to the sum of the effects of its neighbors, the full dynamics is described by

$$\dot{\phi}_i(t) = \omega + \varepsilon \sum_{j \in \mathcal{N}_i} f_{ij}(\phi_j(t - \eta_{ij}) - \phi_i(t)). \quad (2)$$

The function f_{ij} is usually called coupling function, and as before η_{ij} represents delay and \mathcal{N}_i is the set of neighbors of i .

A similar definition for attractive and repulsive couplings can be done in this model. We say that the coupling function f_{ij} is **attractive** if, without delays, the change in speeds brings oscillators closer, and **repulsive** if they are brought apart. Figure 2 shows typical attractive and repulsive coupling functions where arrows represent the speed change produced by the other oscillator; if the pointing direction is counter clockwise, the oscillator speeds up, and otherwise it slows down.

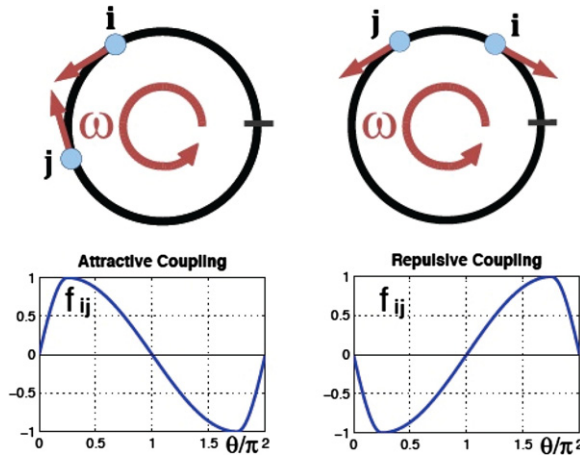


Figure 2. Phase-coupled oscillators with attractive and repulsive coupling. The mutual influence of oscillators i and j is illustrated at the top for both attractive (left) and repulsive (right) coupling. The bottom charts show the corresponding coupling functions.

When $f_{ij} = \frac{K}{N} \sin(\cdot)$, $K > 0$ (attractive coupling), this model is known as the classical Kuramoto model [33]. Intensive research has been conducted on this model, but convergence results are usually limited to cases with all to all coupling ($\mathcal{N}_i = \mathcal{N} \setminus \{i\}$, i.e., complete graph topology) and no delay ($\eta_{ij} = 0$), see e.g. [19, 34], or to some regions of the state space [26].

2.3. Weak coupling approximation

We now concentrate in the regime in which the coupling strength of both models is weak, i.e. $1 \gg \varepsilon > 0$. For pulse-coupled oscillators, this implies that the effect of the jumps originated by each neighbor can be approximated by their average [27]. For phase-coupled oscillators, it implies that to the first order $\phi_i(t - \eta_{ij})$ is well approximated by $\phi_i(t) - \omega\eta_{ij}$.

The effect of these approximations allows us to completely capture the behavior of both systems using the following equation where we assume that every oscillator has the same natural frequency ω and only keep track of the relative difference using

$$\dot{\phi}_i = \varepsilon \sum_{j \in \mathcal{N}_i} f_{ij}(\phi_j - \phi_i - \psi_{ij}). \tag{3}$$

For pulse-coupled oscillators, the coupling function is given by

$$f_{ij}(\theta) = \frac{\omega}{2\pi} \kappa_{ij}(-\theta), \tag{4}$$

and the phase lag $\psi_{ij} = \omega\eta_{ij}$ represents the distance that oscillator i 's phase can travel along the unit circle during the delay time η_{ij} . Equation (4) also shows that the attractive/repulsive coupling classifications of both models are in fact equivalent, since in order to produce the same effect κ_{ij} and f_{ij} should be mirrored, as illustrated in figures 1 and 2.

Equation (3) captures the relative change of the phases and therefore any solution to (3) can be immediately translated to either (1) or (2) by adding ωt . For example, if ϕ^* is an equilibrium of (3), by adding ωt , we obtain a limit cycle in the previous models. Besides the delay interpretation for ψ_{ij} , (3) is also known as a system of coupled oscillators with *frustration*, see e.g. [35].

From now on we will concentrate on (3) with the understanding that any convergence result derived will be immediately true for the original models in the weak coupling limit. We

are interested in the attracting properties of phase-locked invariant orbits within \mathcal{T}^N , which can be represented by $\phi(t) = \omega^* t \mathbf{1}_N + \phi^*$, where $\mathbf{1}_N = (1, \dots, 1)^T \in \mathcal{T}^N$, and ϕ^* and ω^* are solutions to

$$\omega^* = \varepsilon \sum_{j \in \mathcal{N}_i} f_{ij}(\phi_j^* - \phi_i^* - \psi_{ij}), \quad \forall i. \quad (5)$$

Whenever the system reaches one of these orbits, we say that it is synchronized or phase-locked. Additionally, if all the elements of ϕ^* are equal, we say that the system is synchronized **in-phase** or that it is **in-phase** locked. It is easy to check that for a given equilibrium ϕ^* of (3), any solution of the form $\phi^* + \lambda \mathbf{1}_N$, with $\lambda \in \mathbb{R}$, is also an equilibrium that identifies the same limit cycle. Therefore, two equilibria $\phi^{1,*}$ and $\phi^{2,*}$ will be considered to be equivalent, if both identifies the same orbit, or equivalently, if both belongs to the same connected set of equilibria

$$E_{\phi^*} := \{\phi \in \mathcal{T}^N | \phi = \phi^* + \lambda \mathbf{1}_N, \lambda \in \mathbb{R}\}. \quad (6)$$

3. Effect of topology and coupling

In this section we concentrate on the class of coupling functions f_{ij} that are symmetric ($f_{ij} = f_{ji} \forall ij$), odd ($f_{ij}(-\theta) = -f_{ij}(\theta)$) and continuously differentiable. We also assume that there is no delay within the network, i.e. $\psi_{ij} = 0 \forall ij$. Thus, (3) is reduced to

$$\dot{\phi}_i = \varepsilon \sum_{j \in \mathcal{N}_i} f_{ij}(\phi_j - \phi_i). \quad (7)$$

Remark 1. While the continuous differentiable assumption on f_{ij} is technical, the symmetry and odd assumptions have an intuitive interpretation: When f_{ij} is symmetric and odd, the effect of the oscillator j in i ($f_{ij}(\phi_j - \phi_i)$) is equal in magnitude and opposite in sign to the effect of i in j ($f_{ji}(\phi_i - \phi_j)$), i.e. $f_{ij}(\phi_j - \phi_i) = f_{ji}(\phi_j - \phi_i) = -f_{ji}(\phi_i - \phi_j)$. In other words, there is a reciprocity in their mutual effect.

In the rest of this section we progressively show how with some extra conditions on f_{ij} we can guarantee in-phase synchronization for arbitrary undirected graphs. Since we know that the network can have many other phase-locked trajectories besides the in-phase one, our target is an **almost global stability** result [36], meaning that the set of initial conditions that does not eventually lock in phase has zero measure. Later we show how most of the phase-locked solutions that appear on a complete graph are unstable under some general conditions on the structure of the coupling function.

3.1. Preliminaries

We now introduce some prerequisites used in our later analysis.

3.1.1. Algebraic graph theory. We start by reviewing basic definitions and properties from graph theory [37, 38] that are used in the paper. Let G be the connectivity graph that describes the coupling configuration. We use $V(G)$ and $E(G)$ to denote the set of vertices (i or j) and undirected edges (e) of G . An undirected graph G can be directed by giving a specific orientation σ to the elements in the set $E(G)$. That is, for any given edge $e \in E(G)$, we designate one of the vertices to be the *head* and the other one to be the *tail* giving G^σ .

Although in the following definitions we need to give graph G a given orientation σ , the underlying connectivity graph of the system is assumed to be **undirected**. This is not a

problem as the properties used in this paper are independent of a particular orientation σ and they are therefore properties of the undirected graph G . Thus, to simplify notation we drop the superscript σ from G^σ with the understanding that G is now an induced directed graph with some fixed—but arbitrarily chosen—orientation.

We use $P = (V^-, V^+)$ to denote a partition of the vertex set $V(G)$ such that $V(G) = V^- \cup V^+$ and $V^- \cap V^+ = \emptyset$. The cut $C(P)$ associated with P , or equivalently $C(V^-, V^+)$, is defined as $C(P) := \{ij \in E(G) | i \in V^-, j \in V^+, \text{ or vice versa.}\}$. Each partition can be associated with a vector column c_P where $c_P(e) = 1$ if e goes from V^- to V^+ , $c_P(e) = -1$ if e goes from V^+ to V^- and $c_P(e) = 0$ if e stays within either set.

There are several matrices associated with the oriented graph G that embed information about its topology. However, the most significant one for our present work is the *oriented incidence matrix* $B \in \mathbb{R}^{|V(G)| \times |E(G)|}$ where $B(i, e) = 1$ if i is the head of e , $B(i, e) = -1$ if i is the tail of e and $B(i, e) = 0$ otherwise.

3.1.2. Potential dynamics. We now describe how our assumptions on f_{ij} not only simplify the dynamics considerably, but also allow us to use the graph theory properties introduced in section 3.1.1 to gain a deeper understanding of (3).

While f_{ij} being continuously differentiable is standard in order to study local stability and sufficient to apply LaSalle’s invariance principle [39], the symmetry and odd assumptions have a stronger effect on the dynamics.

For example, under these assumptions the system (7) can be compactly rewritten in a vector form as

$$\dot{\phi} = -\varepsilon BF(B^T \phi), \tag{8}$$

where B is the adjacency matrix defined in section 3.1.1 and the map $F : \mathcal{E}(G) \rightarrow \mathcal{E}(G)$ is

$$F(y) = (f_{ij}(y_{ij}))_{ij \in E(G)}.$$

This new representation has several properties. First, from the properties of B one can easily show that (5) can only hold with $\omega^* = 0$ for arbitrary graphs [16] (since $N\omega^* = \omega^* \mathbf{1}_N^T \mathbf{1}_N = -\varepsilon \mathbf{1}_N^T BF(B^T \phi) = 0$), which implies that every phase-locked solution is an equilibrium of (7) and that every limit cycle of the original system (3) can be represented by some E_ϕ^* on (7).

However, the most interesting consequence of (8) comes from interpreting $F(y)$ as the gradient of a potential function

$$W(y) = \sum_{ij \in E(G)} \int_0^{y_{ij}} f_{ij}(s) ds.$$

Then, by defining $V(\phi) = (W \circ B^T)(\phi) = W(B^T \phi)$, (8) becomes a gradient descent law for $V(\phi)$, i.e.,

$$\dot{\phi} = -\varepsilon BF(B^T \phi) = -\varepsilon B \nabla W(B^T \phi) = -\varepsilon \nabla V(\phi),$$

where in the last step above we used the property $\nabla(W \circ B^T)(\phi) = B \nabla W(B^T \phi)$. This makes $V(\phi)$ a natural Lyapunov function candidate since

$$\dot{V}(\phi) = \langle \nabla V(\phi), \dot{\phi} \rangle = -\varepsilon |\nabla V(\phi)|^2 = -\frac{1}{\varepsilon} |\dot{\phi}|^2 \leq 0. \tag{9}$$

Furthermore, since the trajectories of (8) are constrained into the N -dimensional torus \mathcal{T}^N , which is compact, $V(\phi)$ satisfies the hypothesis of LaSalle’s invariance principle (theorem 4.4 [39]), i.e. there is a compact positively invariant set, \mathcal{T}^N and a function $V : \mathcal{T}^N \rightarrow \mathbb{R}$ that decreases along the trajectories $\phi(t)$. Therefore, for every initial condition, the trajectory converges to the largest invariant set M within $\{\dot{V} \equiv 0\}$ which is the equilibria set $E = \{\phi \in \mathcal{T}^N | \dot{\phi} \equiv 0\} = \bigcup_{\phi^*} E_{\phi^*}$.

Remark 2. The fact that symmetric and odd coupling induces potential dynamics is well known in the physics community [40]. However, it has also been rediscovered in the control community [17] for the specific case of sine coupling. Clearly, this does not suffice to show almost global stability, since it is possible to have other stable phase-locked equilibrium sets besides the in-phase one. However, if we can show that all the non-in-phase equilibria are unstable, then almost global stability follows. That is the focus of the next section.

3.2. Negative cut instability condition

We now present the main results of this section. Our technique can be viewed as a generalization of [19]. By means of algebraic graph theory, we provide a better stability analysis of the equilibria under a more general framework. We further use the new stability results to characterize f_{ij} that guarantees almost global stability.

3.2.1. Local stability analysis. In this section we develop the graph theory based tools to characterize the stability of each equilibrium. We will show that given an equilibrium ϕ^* of the system (8), with connectivity graph G and f_{ij} as described in this section, if there exists a cut $C(P)$ such that the sum

$$\sum_{ij \in C(P)} f'_{ij}(\phi_j^* - \phi_i^*) < 0, \tag{10}$$

the equilibrium ϕ^* is **unstable**.

Consider first an equilibrium point ϕ^* . Then, the first order approximation of (8) around ϕ^* is

$$\delta \dot{\phi} = -\varepsilon B \left[\frac{\partial}{\partial y} F(B^T \phi^*) \right] B^T \delta \phi,$$

where $\delta \phi := \phi - \phi^*$ is the incremental phase variable, and $\frac{\partial}{\partial y} F(B^T \phi^*) \in \mathbb{R}^{|E(G)| \times |E(G)|}$ is the Jacobian of $F(y)$ evaluated at $B^T \phi^*$, i.e., $\frac{\partial}{\partial y} F(B^T \phi^*) = \text{diag}(\{f'_{ij}(\phi_j^* - \phi_i^*)\}_{ij \in E(G)})$.

Now let $A = -\varepsilon B \left[\frac{\partial}{\partial y} F(B^T \phi^*) \right] B^T$ and consider the linear system $\delta \dot{\phi} = A \delta \phi$. Although it is possible to numerically calculate the eigenvalues of A given ϕ^* to study the stability, here we use the special structure of A to provide a sufficient condition for instability that has nice graph-theoretical interpretations.

Since A is symmetric, it is straight-forward to check that A has at least one positive eigenvalue, i.e. ϕ^* is unstable, if and only if $x^T A x > 0$. Now, given any partition $P = (V^-, V^+)$, consider the associated vector c_P , define x_P such that $x_i = \frac{1}{2}$ if $i \in V^+$ and $x_i = -\frac{1}{2}$ if $i \in V^-$. Then it follows from the definition of B that $c_P = B^T x_P$ which implies that

$$\frac{-1}{\varepsilon} x_P^T A x_P = c_P^T \left[\frac{\partial}{\partial y} F(B^T \phi^*) \right] c_P = \sum_{ij \in C(P)} f'_{ij}(\phi_j^* - \phi_i^*).$$

Therefore, when condition (10) holds, $A = -\varepsilon B D B^T$ has at least one eigenvalue whose real part is **positive**.

Remark 3. Equation (10) provides a **sufficient** condition for instability; it is not clear what happens when (10) does not hold. However, it gives a graph-theoretical interpretation that can be used to provide stability results for general topologies. That is, if the **minimum cut cost** is negative, the equilibrium is unstable.

Remark 4. Since the weights of the graph $f'_{ij}(\phi_j^* - \phi_i^*)$ are functions of the phase difference, (10) holds for any equilibria of the form $\phi^* + \lambda \mathbf{1}_N$. Thus, the result holds for the whole set E_{ϕ^*} defined in (6).

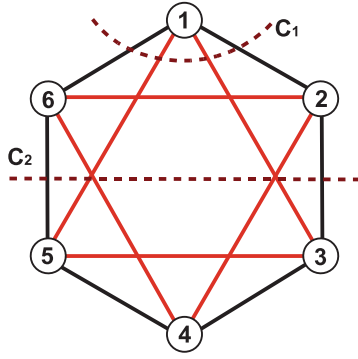


Figure 3. The network of six oscillators (example 4).

When (10) is specialized to $P = (\{i\}, V(G)\setminus\{i\})$ and $f_{ij}(\theta) = \sin(\theta)$, it reduces to the instability condition in lemma 2.3 of [19]; i.e.,

$$\sum_{j \in \mathcal{N}_i} \cos(\phi_j^* - \phi_i^*) < 0. \tag{11}$$

However, (10) has a broader applicability spectrum as shown in the following example.

Example 1. Consider a six oscillators network as in figure 3, where each node is linked to its four closest neighbors and $f_{ij}(\theta) = \sin(\theta)$. Then, by symmetry, it is easy to verify that

$$\phi^* = \left[0, \frac{\pi}{3}, \frac{2\pi}{3}, \pi, \frac{4\pi}{3}, \frac{5\pi}{3} \right]^T \tag{12}$$

is an equilibrium of (7).

We first study the stability of ϕ^* using (11) as in [19]. By substituting (12) in $\cos(\phi_j^* - \phi_i^*) \forall i, j \in E(G)$ we find that the edge weights can only take two values:

$$\cos(\phi_j^* - \phi_i^*) = \begin{cases} \cos\left(\frac{\pi}{3}\right) = \frac{1}{2}, & \text{if } j = i \pm 1 \pmod 6 \\ \cos\left(\frac{2\pi}{3}\right) = -\frac{1}{2}, & \text{if } j = i \pm 2 \pmod 6 \end{cases}.$$

Then, since any cut that isolates one node from the rest (like $C_1 = C(\{1\}, V(G)\setminus\{1\})$ in figure 3) will always have two edges of each type, their sum is **zero**. Therefore, (11) cannot be used to determine stability.

If we now use condition (10) instead, we can explore a wider variety of cuts that can potentially have smaller costs. In fact, if instead of C_1 we sum over $C_2 = C(\{1, 2, 6\}, \{3, 4, 5\})$, we obtain,

$$\sum_{ij \in C_2} \cos(\phi_j^* - \phi_i^*) = -1 < 0,$$

which implies that ϕ^* is unstable.

Figure 4 verifies the equilibrium instability. By starting with an initial condition $\phi_0 = \phi^* + \delta\phi$ close to the equilibrium ϕ^* , we can see how the system slowly starts to move away from ϕ^* towards a **stable** equilibrium set.

Furthermore, we can study the whole family of non-isolated equilibria given by

$$\phi^* = \left[\varepsilon_1, \frac{\pi}{3} + \varepsilon_2, \frac{2\pi}{3} + \varepsilon_3, \pi + \varepsilon_1, \frac{4\pi}{3} + \varepsilon_2, \frac{5\pi}{3} + \varepsilon_3 \right]^T \tag{13}$$

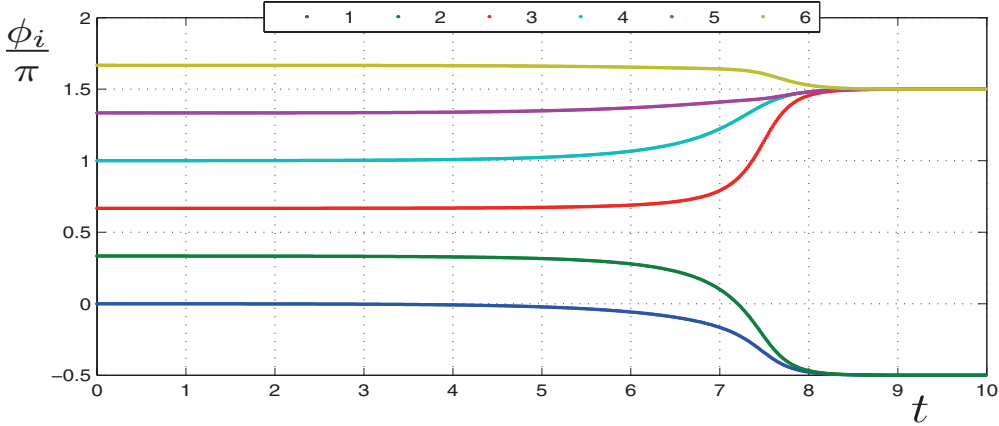


Figure 4. Unstable equilibrium ϕ^* . Initial condition $\phi_0 = \phi^* + \delta p$, where δp is a small perturbation. The small perturbation gets amplified showing that the equilibrium is unstable.

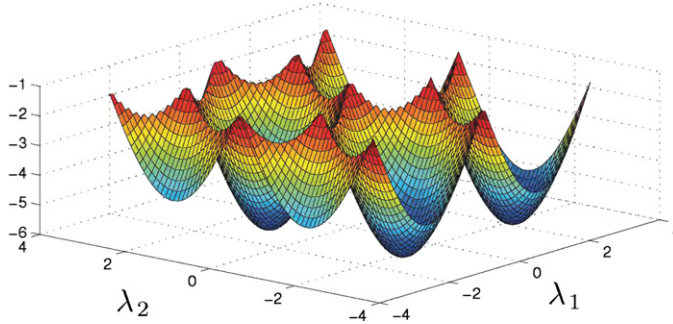


Figure 5. Minimum cut value $C^*(\lambda_1, \lambda_2)$ showing that the equilibria (13) are unstable.

where $\varepsilon_1, \varepsilon_2, \varepsilon_3 \in \mathbb{R}$, which due to remark 4, we can reduce (13) to

$$\phi^* = \left[0, \frac{\pi}{3} + \lambda_1, \frac{2\pi}{3} + \lambda_2, \pi, \frac{4\pi}{3} + \lambda_1, \frac{5\pi}{3} + \lambda_2 \right]^T \tag{14}$$

with $\lambda_1 = \varepsilon_2 - \varepsilon_1$ and $\lambda_2 = \varepsilon_3 - \varepsilon_1$.

Instead of focusing on only one cut, here we compute the minimum cut value (10) over the 31 possible cuts, i.e. $C^*(\lambda_1, \lambda_2) := \min_P \sum_{ij \in C(P)} f'_{ij}(\phi_j(\lambda_1, \lambda_2)^* - \phi_i^*(\lambda_1, \lambda_2))$. Figure 5 shows the value of $C^*(\lambda_1, \lambda_2)$ for $\lambda_i \in [-\pi, \pi]$. Since $C^*(\lambda_1, \lambda_2)$ is 2π -periodic on each variable and its value is negative for every $\lambda_1, \lambda_2 \in [-\pi, \pi]$, the family of equilibria (14) (and consequently (13)) is unstable.

3.2.2. Almost global stability. Condition (10) also provides insight on which class of coupling functions can potentially give us almost global convergence to the in-phase equilibrium set E_{1_N} . If it is possible to find some f_{ij} with $f'_{ij}(0) > 0$, such that for any non-in-phase equilibrium ϕ^* , there is a cut C with $\sum_{ij \in C} f'_{ij}(\phi_j^* - \phi_i^*) < 0$, then the in-phase equilibrium set will be almost globally stable [13]. The main difficulty is that for general f_{ij} and arbitrary network G , it is not easy to locate every phase-locked equilibria and it is therefore not simple to know in what region of the domain of f_{ij} the slope should be negative.

We now concentrate on the one-parameter family of functions \mathcal{F}_b , with $b \in (0, \pi)$, such that $f_{ij} \in \mathcal{F}_b$ whenever f_{ij} is **symmetric, odd, continuously differentiable** and

- $f'_{ij}(\theta; b) > 0, \forall \theta \in (0, b) \cup (2\pi - b, 2\pi)$, and
- $f'_{ij}(\theta; b) < 0, \forall \theta \in (b, 2\pi - b)$.

See figure 2 for an illustration with $b = \frac{\pi}{4}$. Also note that this definition implies that if $f_{ij}(\theta; b) \in \mathcal{F}_b$, the coupling is attractive and $f_{ij}(\theta; b) > 0 \forall \theta \in (0, \pi)$. This last property will be used later. We also assume the graph G to be **connected**.

In order to obtain almost global stability we need b to be small. However, since the equilibria position is not known *a priori*, it is not clear how small b should be or if there is any $b > 0$ such that all non-trivial equilibria are unstable. Therefore, we first need to estimate the region of the state space that contains every non-trivial phase-locked solution.

Let I be a compact connected subset of \mathbb{S}^1 and let $l(I)$ be its length, e.g., if $I = \mathbb{S}^1$ then $l(I) = 2\pi$. For any $S \subset V(G)$ and $\phi \in \mathcal{T}^N$, define $d(\phi, S)$ as the length of the smallest interval I such that $\phi_i \in I \forall i \in S$, i.e.

$$d(\phi, S) = l(I^*) = \min_{I: \phi_i \in I, \forall i \in S} l(I).$$

Using this metric, together with the aid of theorem 2.6 of [16], we can identify two very insightful properties of the family \mathcal{F}_b whenever the graph G is connected.

Lemma 1. *If ϕ^* is an equilibrium point of (8) with $d(\phi^*, V(G)) \leq \pi$, then either ϕ^* is an in-phase equilibrium, i.e. $\phi^* = \lambda \mathbf{1}_N$ for $\lambda \in \mathbb{R}$, or has a cut C with $f'_{ij}(\phi_j^* - \phi_i^*) < 0 \forall ij \in C$.*

Proof. Since $d(\phi^*, V(G)) \leq \pi$, all the phases are contained in a half circle and for the oscillator with smallest phase i_0 , all the phase differences $(\phi_j^* - \phi_{i_0}^*) \in [0, \pi]$. However, since $f_{ij}(\cdot; b) \in \mathcal{F}_b$ implies $f_{ij}(\theta; b) \geq 0 \forall \theta \in [0, \pi]$ with equality only for $\theta \in \{0, \pi\}$, $\dot{\phi}_{i_0}^* = \sum_{j \in \mathcal{N}_{i_0}} f_{ij}(\phi_j^* - \phi_{i_0}^*) = 0$ can only hold if $\phi_j^* - \phi_{i_0}^* \in \{0, \pi\} \forall j \in \mathcal{N}_{i_0}$. Now let $V^- = \{i \in V(G) : d(\phi^*, \{i, i_0\}) = 0\}$ and $V^+ = V(G) \setminus V^-$. If $V^- = V(G)$, then ϕ^* is an in-phase equilibrium. Otherwise, $\forall ij \in C(V^-, V^+)$, $f'_{ij}(\phi_j^* - \phi_i^*) = f'_{ij}(\pi) < 0$. \square

We are now ready to establish a bound on the value of b that guarantees the instability of the non-in-phase equilibria.

Lemma 2. *Consider $f_{ij}(\cdot; b) \in \mathcal{F}_b \forall ij \in E(G)$ and arbitrary connected (undirected) graph G . Then, for any $b \leq \frac{\pi}{N-1}$ and non-in-phase equilibrium ϕ^* , there is a cut C with $f'_{ij}(\phi_j^* - \phi_i^*; b) < 0, \forall ij \in C$*

Proof. Suppose there is a non-in-phase equilibrium ϕ^* for which no such cut C exists. Let $V_0^- = \{i_0\}$ and $V_0^+ = V(G) \setminus \{i_0\}$ be a partition of $V(G)$ for some arbitrary node i_0 .

Since such C does not exist, there is some edge $i_0 j_1 \in C(V_0^-, V_0^+)$, with $j_1 \in V_0^+$, such that $f'_{i_0 j_1}(\phi_{j_1}^* - \phi_{i_0}^*; b) \geq 0$. Move j_1 from one side to the other of the partition by defining $V_1^- := V_0^- \cup \{j_1\}$ and $V_1^+ := V_0^+ \setminus \{j_1\}$. Now since $f'_{i_0 j_1}(\phi_{j_1}^* - \phi_{i_0}^*; b) \geq 0$, then

$$d(\phi^*, V_1^-) \leq b.$$

In other words, both phases should be within a distance smaller than b .

Now repeat the argument k times. At the k th iteration, given V_{k-1}^-, V_{k-1}^+ , again we can find some $i_{k-1} \in V_{k-1}^-, j_k \in V_{k-1}^+$ such that $i_{k-1} j_k \in C(V_{k-1}^-, V_{k-1}^+)$ and $f'_{i_{k-1} j_k}(\phi_{j_k}^* - \phi_{i_{k-1}}^*; b) \geq 0$. Also, since at each step $d(\phi^*, \{i_{k-1}, j_k\}) \leq b$,

$$d(\phi^*, V_k^-) \leq b + d(\phi^*, V_{k-1}^-).$$

Thus by solving the recursion we get: $d(\phi^*, V_k^-) \leq kb$.

After $N - 1$ iterations we have $V_{N-1}^- = V(G)$ and $d(\phi^*, V(G)) \leq (N - 1)b$. Therefore, since $b \leq \frac{\pi}{N-1}$, we obtain

$$d(\phi^*, V(G)) \leq (N - 1) \frac{\pi}{N - 1} = \pi.$$

Then, by lemma 1 ϕ^* is either an in-phase equilibrium or there is a cut C with $f'_{ij}(\phi_j^* - \phi_i^*) < 0 \forall ij \in C$. Either case gives a contradiction to assuming that ϕ^* is a non-in-phase equilibrium and C does not exist. Therefore, for any non-in-phase ϕ^* and $b \leq \frac{\pi}{N-1}$, we can always find a cut C with $f'_{ij}(\phi_j^* - \phi_i^*; b) < 0, \forall ij \in C$. \square

Lemma 2 allows us to use our cut condition (10) on every non-in-phase equilibrium. Thus, since (8) is a potential dynamics (cf section 3.1.2), from every initial condition the system converges to the set of equilibria E . But when $b \leq \frac{\pi}{N-1}$ the only stable equilibrium set inside E is the in-phase set E_{1_N} . Thus, E_{1_N} set is globally asymptotically stable. We have summarized this result in the following theorem.

Theorem 1 (Almost global stability). *Consider $f_{ij}(\theta; b) \in \mathcal{F}_b$ and an arbitrary connected graph G . Then, if $b \leq \frac{\pi}{N-1}$, the in-phase equilibrium set E_{1_N} is **almost globally asymptotically stable**.*

This result provides a sufficient condition for almost global asymptotic stability to the in-phase equilibrium set E_{1_N} . Although found independently, the same condition was proposed for a specific piecewise linear f_{ij} in [41]. Here we extend [41] in many aspects. For example, instead of assuming equal coupling for every edge, our condition describes a large family of coupling functions \mathcal{F}_b where each f_{ij} can be taken independently from \mathcal{F}_b . Also, in [41] the construction of $f_{ij}(\theta)$ assumes a discontinuity on the derivative at $\theta = b$. This can pose a problem if the equilibrium ϕ^* happens to have phase differences $\phi_j^* - \phi_i^* = b$. Here we do not have this problem as f_{ij} is continuously differentiable.

The condition $b \leq \frac{\pi}{N-1}$ implies that, when N is large, f_{ij} should be decreasing in most of its domain. Using (4) this implies that κ_{ij} should be increasing within the region $(b, 2\pi - b)$, which is similar to the condition on [20] and equivalent when $b \rightarrow 0$. Thus, theorem 1 confirms the conjecture of [20] by extending their result to arbitrary topologies and a more realistic continuous κ_{ij} for the system (1) in the weak coupling limit.

3.3. Complete graph topology with a class of coupling functions

In this subsection, we investigate how conservative the value of b found in section 3.2.2 is for the complete graph topology. We are motivated by the results of [19] which show that $f(\theta) = \sin(\theta)$ ($b = \frac{\pi}{2}$) with complete graph topology ensures almost global synchronization.

Since for general f it is not easy to characterize all the possible system equilibria, we study the stability of the equilibria that appear due to the equivalence of (8) with respect to the action group $S_N \times T^1$, where S_N is the group of permutations of the N coordinates and $T^1 = [0, 2\pi)$ represents the group action of phase shift of all the coordinates, i.e. the action of $\delta \in T^1$ is $\phi_i \mapsto \phi_i + \delta \forall i$. Readers should refer to [12, 16] for a detailed study of the effect of this property.

These equilibria are characterized by the isotropy subgroups Γ of $S_N \times T^1$ that keep them fixed, i.e., $\gamma\phi^* = \phi^* \forall \gamma \in \Gamma$. In [12] it was shown that this isotropy subgroups take the form of

$$(S_{k_0} \times S_{k_1} \times \dots \times S_{k_{l_B-1}})^m \rtimes Z_m$$

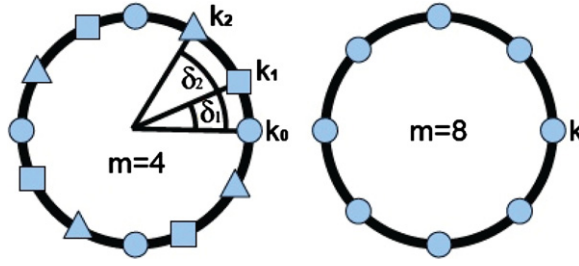


Figure 6. Equilibria with isotropy $(S_{k_0} \times S_{k_1} \times S_{k_2})^4 \rtimes Z_4$ (left) and $(S_k)^8 \rtimes Z_8$ (right).

where k_i and m are positive integers such that $(k_0 + k_1 + \dots + k_{l_B-1})m = N$, S_j is the permutation subgroup of S_N of j -many coordinates and Z_m is the cyclic group with action $\phi_i \mapsto \phi_i + \frac{2\pi}{m}$. The semi-product \rtimes represents the fact that Z_m does not commute with the other subgroups.

In other words, each equilibria with isotropy $(S_{k_0} \times S_{k_1} \times \dots \times S_{k_{l_B-1}})^m \rtimes Z_m$ is conformed by l_B shifted constellations C_l ($l \in \{0, 1, \dots, l_B - 1\}$) of m evenly distributed blocks, with k_l oscillators per block. We use δ_l to denote the phase shift between constellation C_0 and C_l . See figure 6 for examples of these types of equilibria.

Here we will show that under mild assumptions on f and for $b = \frac{\pi}{2}$ most of the equilibria found with these characteristics are unstable. We first study all the equilibria with m even. In this case, there is a special property that can be exploited.

That is, when $f \in \mathcal{F}_{\frac{\pi}{2}}$ such that f is even around $\frac{\pi}{2}$, we have

$$\begin{aligned}
 g_m(\delta) &:= \sum_{j=0}^{m-1} f\left(\frac{2\pi}{m}j + \delta\right) \\
 &= \sum_{j=0}^{m/2-1} f\left(\frac{2\pi}{m}j + \delta\right) + f\left(\pi + \frac{2\pi}{m}j + \delta\right) \\
 &= \sum_{j=0}^{m/2-1} f\left(\frac{2\pi}{m}j + \delta\right) + f\left(\left(\frac{3\pi}{2} + \frac{2\pi}{m}j + \delta\right) - \frac{\pi}{2}\right) \\
 &= \sum_{j=0}^{m/2-1} f\left(\frac{2\pi}{m}j + \delta\right) + f\left(-\left(\frac{2\pi}{m}j + \delta\right)\right) \\
 &= \sum_{j=0}^{m/2-1} f\left(\frac{2\pi}{m}j + \delta\right) - f\left(\frac{2\pi}{m}j + \delta\right) = 0
 \end{aligned} \tag{15}$$

where the third step comes from f being even around $\pi/2$ and 2π -periodic, and the fourth from f being odd.

Having $g_m(\delta) = 0$ is the key to prove the instability of every equilibria with even m . It essentially states that the aggregate effect of one constellation C_l on any oscillator $j \in V(G) \setminus C_l$ is zero when m is even, and therefore any perturbation that maintains C_l has null effect on j . This is shown in the next proposition.

Theorem 2 (Instability for even m). *Given an equilibrium ϕ^* with isotropy $(S_{k_1} \times S_{k_2} \times \dots \times S_{k_{l_B}})^m \rtimes Z_m$ and $f \in \mathcal{F}_{\frac{\pi}{2}}$ even around $\frac{\pi}{2}$. Then, if m is even, ϕ^* is unstable.*

Proof. We will show the instability of ϕ^* by finding a cut of the network satisfying (10). Let $V_0 \subset V(G)$ be the set of nodes within one of the blocks of the constellation C_0 and consider

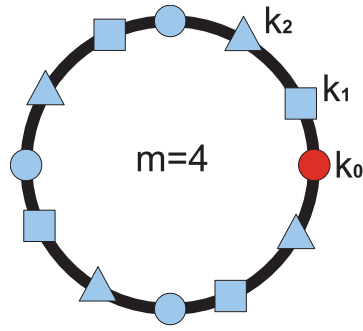


Figure 7. Cut of theorem 2, the red block represents one possible set V_0 .

the partition induced by V_0 as shown in figure 7, i.e. $P = (V_0, V(G) \setminus V_0)$. Due to the structure of ϕ^* , (10) becomes

$$\sum_{ij \in C(P)} f'(\phi_j^* - \phi_i^*) = -k_1 f'(0) + \sum_{l=1}^{l_B} k_l g'_m(\delta_l),$$

where $g'_m(\delta)$ is the derivative of g_m and δ_l is the phase shift between the C_0 and C_l . Finally, since by assumptions $g_m(\delta) \equiv 0 \forall \delta$ it follows that $g'_m(\delta) \equiv 0$ and

$$\sum_{ij \in C(P)} f'_{ij}(\phi_j^* - \phi_i^*) = -k_1 f'(0) < 0.$$

Therefore, by (10), ϕ^* is unstable. □

The natural question that arises is whether similar results can be obtained for m odd. The main difficulty in this case is that $g_m(\delta) = 0$ does not hold since we no longer evaluate f at points with phase difference equal to π such that they cancel each other. Therefore, an extra monotonicity condition needs to be added in order to partially answer this question. These conditions and their effects are summarized in the following claims.

Lemma 3 (Monotonicity). *Given $f \in \mathcal{F}_{\frac{\pi}{2}}$ such that f is strictly concave for $\theta \in [0, \pi]$, then*

$$f'(\theta) - f'(\theta - \phi) < 0, \quad 0 \leq \theta - \phi < \theta \leq \pi \tag{16}$$

$$f'(\theta) - f'(\theta + \phi) < 0, \quad -\pi \leq \theta < \theta + \phi \leq 0. \tag{17}$$

Proof. The proof is a direct consequence of the strict concavity of f . Since $f(\theta)$ is strictly concave, then basic convex analysis shows that $f'(\theta)$ is strictly decreasing within $[0, \pi]$. Therefore, the inequality (16) follows directly from the fact that $\theta \in [0, \pi], \theta - \phi \in [0, \pi]$ and $\theta - \phi < \theta$. To show (17) it suffices to notice that since f is odd ($f \in \mathcal{F}_{\frac{\pi}{2}}$), f is strictly convex in $[\pi, 2\pi]$. The rest of the proof is analogous to (16). □

Lemma 4 (f' Concavity). *Given $f \in \mathcal{F}_{\frac{\pi}{2}}$ such that f' is strictly concave for $\theta \in [-\frac{\pi}{2}, \frac{\pi}{2}]$. Then for all $m \geq 4$, $f'(\frac{\pi}{m}) \geq \frac{1}{2} f'(0)$.*

Proof. Since $f'(\theta)$ is concave for $\theta \in [-\pi, \pi]$ then it follows

$$f'\left(\frac{\pi}{m}\right) = f'\left(\lambda_m 0 + (1 - \lambda_m) \frac{\pi}{2}\right) > \lambda_m f'(0) + (1 - \lambda_m) f'\left(\frac{\pi}{2}\right) > \lambda_m f'(0)$$

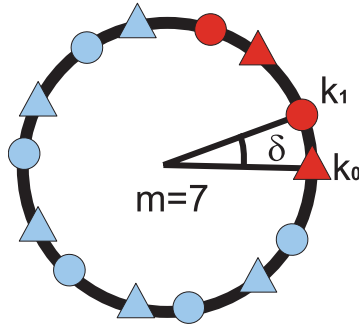


Figure 8. Cut used in theorem 3. The dots in red represent all the oscillators of some maximal set S with $d(\phi^*, S) < \frac{4\pi}{m}$.

where $\lambda_m = \frac{m-2}{m}$. Thus, for $m \geq 4$, $\lambda_m \geq \frac{1}{2}$ and

$$f' \left(\frac{\pi}{m} \right) > \frac{1}{2} f'(0)$$

as desired. □

Now we show the instability of any equilibria with isotropy $(S_{k_1} \times S_{k_2} \times \dots \times S_{k_B})^m \times Z_m$ for m odd and greater or equal to 7.

Theorem 3 (Instability for $m \geq 7$ and odd). *Suppose $f \in \mathcal{F}_{\frac{\pi}{2}}$ with f concave in $[0, \pi]$ and f' concave in $[-\frac{\pi}{2}, \frac{\pi}{2}]$, then for all $m = 2k + 1$ with $k \geq 3$ the equilibria ϕ^* with isotropy $(S_{k_1} \times S_{k_2} \times \dots \times S_{k_B})^m \times Z_m$ are unstable.*

Proof. As in theorem 2 we will use our cut condition to show the instability of ϕ^* . Thus, we define a partition $P = (S, V(G) \setminus S)$ of $V(G)$ by taking S to be a maximal subset of $V(G)$ such that $d(\phi, S) < \frac{4\pi}{m}$, see figure 8 for an illustration of P . Notice that any of these partitions will include all the oscillators of two consecutive blocks of every constellation.

Instead of evaluating the total sum of the weights in the cut, we will show that the sum of edge weights of the links connecting the nodes of one constellation in S with the nodes of a possibly different constellation in $V(G) \setminus S$ is negative. In other words, we will focus on showing

$$\sum_{ij \in \mathcal{K}_{l_1 l_2}} f'(\phi_j^* - \phi_i^*) < 0 \tag{18}$$

where $\mathcal{K}_{l_1 l_2} = \{ij : i \in C_{l_1} \cap S, j \in C_{l_2} \cap V(G) \setminus S\}$.

Given any subset of integers J , we define

$$g_m^J(\delta) = g_m(\delta) - \sum_{j \in J} f \left(\frac{2\pi}{m} j + \delta \right).$$

Then, we can rewrite (18) as

$$\begin{aligned} \sum_{ij \in \mathcal{K}_{l_1 l_2}} f'(\phi_j^* - \phi_i^*) &= (g_m^{(0,1)})'(\delta_{l_1 l_2}) + (g_m^{(-1,0)})'(\delta_{l_1 l_2}) \\ &= 2g_m'(\delta_{l_1 l_2}) - f' \left(\delta_{l_1 l_2} + \frac{2\pi}{m} \right) - 2f'(\delta_{l_1 l_2}) - f' \left(\delta_{l_1 l_2} - \frac{2\pi}{m} \right) \end{aligned} \tag{19}$$

where $\delta_{l_1 l_2} \in [0, \frac{2\pi}{m}]$ is the phase shift between the two constellations. Then, if we can show that for all $\delta \in [0, \frac{2\pi}{m}]$ (19) is less than zero, for any values of l_1 and l_2 , (18) will be satisfied.

Since f is odd and even around $\frac{\pi}{2}$, f' is even and odd around $\frac{\pi}{2}$ and $g'_m(\delta)$ can be rewritten as

$$g'_m(\delta) = f'(\delta) + \sum_{1 \leq |j| \leq \lfloor \frac{k}{2} \rfloor} \left\{ f' \left(\delta + \frac{2\pi}{m} j \right) - f' \left(\delta - \operatorname{sgn}(j) \frac{\pi}{m} + \frac{2\pi}{m} j \right) \right\} - \left[f' \left(\delta + \frac{\pi}{m} k \right) + f' \left(\delta - \frac{\pi}{m} k \right) \right] \mathbf{1}_{[k \text{ odd}]}$$

where $\mathbf{1}_{[k \text{ odd}]}$ is the indicator function of the event $[k \text{ odd}]$, the sum is over all the integers j with $1 \leq |j| \leq \lfloor \frac{k}{2} \rfloor$ and $k = \frac{m-1}{2}$.

The last term only appears when k is odd and in fact it is easy to prove that it is always negative, as shown in the following calculation:

$$\begin{aligned} -f' \left(\delta + \frac{\pi}{m} k \right) - f' \left(\delta - \frac{\pi}{m} k \right) &= -f' \left(\frac{\pi}{m} k + \delta \right) - f' \left(\frac{\pi}{m} k - \delta \right) \\ &= -f' \left(\frac{\pi}{2} - \frac{\pi}{2m} + \delta \right) - f' \left(\frac{\pi}{2} - \frac{\pi}{2m} - \delta \right) \\ &= f' \left(\frac{\pi}{2} - \delta + \frac{\pi}{2m} \right) - f' \left(\frac{\pi}{2} - \delta - \frac{\pi}{2m} \right) \\ &= f'(\theta) - f'(\theta - \phi) < 0 \end{aligned}$$

where in step one we used the fact of f' being even, in step two we used $k = \frac{m-1}{2}$ and in step three we used f' being odd around $\frac{\pi}{2}$. The last step comes from substituting $\theta = \frac{\pi}{2} - \delta + \frac{\pi}{2m}$, $\phi = \frac{\pi}{m}$ and applying lemma 3, since for $m \geq 7$ we have $0 \leq \theta - \phi < \theta \leq \pi$.

Then it remains to show that the terms of the form $f'(\delta + \frac{2\pi}{m} j) - f'(\delta - \operatorname{sgn}(j) \frac{\pi}{m} + \frac{2\pi}{m} j)$ are negative for all j s.t. $1 \leq |j| \leq \lfloor \frac{k}{2} \rfloor$. This is indeed true when j is positive since for all $\delta \in [0, \frac{2\pi}{m}]$ we get

$$0 \leq \delta - \frac{\pi}{m} + \frac{2\pi}{m} j < \delta + \frac{2\pi}{m} j \leq \pi, \quad \text{for } 1 \leq j \leq \left\lfloor \frac{k}{2} \right\rfloor$$

and thus we can apply again lemma 3.

When j is negative, there is one exception in which lemma 3 cannot be used since

$$-\pi \leq \delta + \frac{2\pi}{m} j < \delta + \frac{2\pi}{m} j + \frac{\pi}{m} \leq 0, \quad \forall \delta \in \left[0, \frac{2\pi}{m} \right]$$

only holds for $-\lfloor \frac{k}{2} \rfloor \leq j \leq -2$. Thus, the term corresponding to $j = -1$ cannot be directly eliminated.

Therefore, by keeping only the terms of the sum with $j = \pm 1$, g'_m is strictly upper bounded for all $\delta \in [0, \frac{2\pi}{m}]$ by

$$g'_m(\delta) < f'(\delta) + f' \left(\delta - \frac{2\pi}{m} \right) - f' \left(\delta - \frac{\pi}{m} \right) + f' \left(\delta + \frac{2\pi}{m} \right) - f' \left(\delta + \frac{\pi}{m} \right). \tag{20}$$

Now, substituting (20) in (19) we get

$$\begin{aligned} \sum_{ij \in \mathcal{K}_{i_1 i_2}} f'(\phi_j^* - \phi_i^*) &< f' \left(\delta - \frac{2\pi}{m} \right) - 2f' \left(\delta - \frac{\pi}{m} \right) + f' \left(\delta + \frac{2\pi}{m} \right) - 2f' \left(\delta + \frac{\pi}{m} \right) \\ &\leq f' \left(\delta - \frac{2\pi}{m} \right) - 2f' \left(\delta - \frac{\pi}{m} \right) - f' \left(\delta + \frac{\pi}{m} \right) \\ &\leq f' \left(\delta - \frac{2\pi}{m} \right) - 2f' \left(\delta - \frac{\pi}{m} \right) \end{aligned}$$

where in the last step we used the fact that for $m \geq 6$ and $\delta \in [0, \frac{2\pi}{m}]$, $f'(\delta + \frac{\pi}{m}) \geq 0$.

Finally, since for $\delta \in [0, \frac{2\pi}{m}]$ $f'(\delta - \frac{2\pi}{m})$ is strictly increasing and $f'(\delta - \frac{\pi}{m})$ achieves its minimum for $\delta \in \{0, \frac{2\pi}{m}\}$, then

$$f' \left(\delta - \frac{2\pi}{m} \right) - 2f' \left(\delta - \frac{\pi}{m} \right) \leq f'(0) - 2f' \left(\frac{\pi}{m} \right) \leq 0$$

where the last inequality follows from lemma 4.

Therefore, for all m odd greater or equal to 7 we obtain

$$\sum_{ij \in \mathcal{K}_{l_1 l_2}} f'(\phi_j^* - \phi_i^*) < f'(0) - 2f' \left(\frac{\pi}{m} \right) \leq 0$$

and since this result is independent on the indices l_1, l_2 , then

$$\sum_{ij \in C(S, V(G) \setminus S)} f'(\phi_j^* - \phi_i^*) = \sum_{l_1=1}^{l_B} \sum_{l_2=1}^{l_B} \sum_{ij \in \mathcal{K}_{l_1 l_2}} f'(\phi_j^* - \phi_i^*) < 0$$

and thus ϕ^* is unstable. □

4. Effect of delay

In this section, we study how delay can *change* the stability in a network of weakly coupled oscillators. Using mean field theory, we construct a non-delayed system with the same continuum limit. This allows us to use our instability cut condition as well as other tools available in the literature to study the effect of heterogeneous delays on the system's behavior. In particular, we show that for Kuramoto oscillators heterogeneous and homogeneous delays are equivalent, and that large heterogeneous delays can help reach synchronization, which are both a bit counterintuitive conclusions. Our analysis significantly generalizes previous related studies for general coupling functions [28, 42, 43] and complements the study of Kuramoto oscillators in [44, 45] by characterizing the parameters of the delay distribution that define the behavior of the system when the frequencies are homogeneous.

Once delay is introduced in the system of coupled oscillators, the problem becomes fundamentally harder. For example, for pulse-coupled oscillators, the reception of a pulse no longer gives accurate information about the relative phase difference $\Delta\phi_{ij} = \phi_j - \phi_i$ between the two interacting oscillators. Before, at the exact moment when i received a pulse from j , ϕ_j was zero and the phase difference was estimated locally by i as $\Delta\phi_{ij} = -\phi_i$. However, now when i receives the pulse, the difference becomes $\Delta\phi_{ij} = -\phi_i - \psi_{ij}$. Therefore, the delay propagation acts as an error introduced in the phase difference measurement and unless some information is known about this error, it is impossible to predict the behavior. Moreover, as we will see later, slight changes in the distribution can produce nonintuitive behaviors.

We will consider the case where the coupling between oscillators is all to all and identical ($\mathcal{N}_i = \mathcal{N} \setminus \{i\}, \forall i \in \mathcal{N}$ and $f_{ij} = f \forall i, j$). And assume the phase lags ψ_{ij} are randomly and independently chosen from the same distribution with probability density $g(\psi)$. By letting $N \rightarrow +\infty$ and $\varepsilon \rightarrow 0$ while keeping $\varepsilon N =: \bar{\varepsilon}$ a constant, (3) becomes

$$v(\phi, t) := \omega + \bar{\varepsilon} \int_{-\pi}^{\pi} \int_0^{+\infty} f(\sigma - \phi - \psi) g(\psi) \rho(\sigma, t) d\psi d\sigma, \tag{21}$$

where $\rho(\phi, t)$ is a time-variant normalized phase distribution that keeps track of the fraction of oscillators with phase ϕ at time t , and $v(\phi, t)$ is the velocity field that expresses the net force that the whole population applies to a given oscillator with phase ϕ at time t . Since the number of oscillators is preserved at any time, the evolution of $\rho(\phi, t)$ is governed by the continuity equation

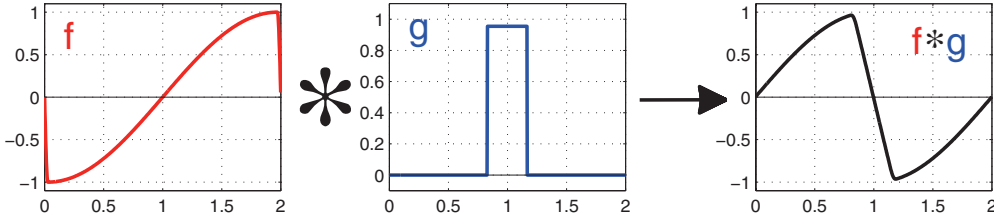


Figure 9. Effect of delay in coupling shape. The delay distribution g modifies the shape of the coupling function H of the equivalent system (23) according to (24). This has a significant impact on the behavior of the system.

$$\frac{\partial}{\partial t} \rho(\phi, t) + \frac{\partial}{\partial \phi} (\rho(\phi, t)v(\phi, t)) = 0 \tag{22}$$

with the boundary conditions $\rho(0, t) \equiv \rho(2\pi, t)$.

Equations (21)–(22) are not analytically solvable for general f and g . Therefore, instead of studying (21)–(22), here we use a different strategy. We consider the non-delayed system of the form

$$\dot{\phi}_i = \omega + \varepsilon \sum_{j \in \mathcal{N}_i} H(\phi_j - \phi_i), \tag{23}$$

where

$$H(\theta) = (f * g)(\theta) = \int_0^{+\infty} f(\theta - \psi)g(\psi) d\psi \tag{24}$$

is the convolution between f and g .

Although (23) is quite different from (3) and thus has a different behavior, both systems **have the same continuum limit** since the velocity field of (23) is given by

$$\begin{aligned} v_H(\phi, t) &= \omega + \bar{\varepsilon} \int_0^{2\pi} H(\sigma - \phi)\rho(\sigma, t) d\sigma \\ &= \omega + \bar{\varepsilon} \int_0^{2\pi} \left(\int_0^{+\infty} f((\sigma - \phi) - \psi)g(\psi) d\psi \right) \rho(\sigma, t) d\sigma \\ &= v(\phi, t), \end{aligned}$$

where in the first and second steps we used (24) and (21) respectively. Therefore, as N grows, (23) starts to become a good approximation of (3) and therefore can be analyzed to understand the behavior of (3).

Equations (23)–(24) also unveil the significant impact that the delay distribution may have in the system. For example, figure 9 shows how the underlying delay (in this case the delay distribution) determines what type of coupling (attractive or repulsive) produces synchronization. The original function f produces repulsive coupling, whereas the corresponding H is attractive. In fact, as we will soon see, the distribution of delay can not only qualitatively affect the type of coupling but it can also modify the stability of certain phase-locked limit cycles. In the rest of this section, we will use the system (23) to study the effect of heterogeneous delays on (3). Our analysis builds on the local stability analysis of section 3 and the analysis of non-delayed coupled oscillators in [46]. We also provide numerical simulations to verify our predictions.

4.1. Kuramoto oscillators

We first consider the effect of delay when $f(\theta) = K \sin(\theta)$, i.e. when (3) is the Kuramoto model [14]. Although this problem has been intensively studied [44, 45, 47, 48] for the heterogeneous

frequency case using a local stability analysis on (22), our approach unveils new significant implications. We show that when the frequencies are homogeneous, the Kuramoto model with heterogenous delays can be reduced to the homogeneous delay case with possibly different coupling gain. This has been numerically observed in [44] but not theoretically proved. Moreover, we characterize the unique two parameters of the delay distribution that govern the global behavior of the system.

We begin by computing (24). When $f(\theta) = K \sin(\theta)$, $H(\theta)$ can be easily calculated:

$$\begin{aligned} H(\theta) &= \int_0^{+\infty} K \sin(\theta - \psi) g(\psi) d\psi \\ &= K \int_0^{+\infty} \Im[e^{i(\theta-\psi)} g(\psi)] d\psi = K \Im \left[e^{i\theta} \int_0^{+\infty} e^{-i\psi} g(\psi) d\psi \right] \\ &= K \Im[e^{i\theta} C e^{-i\xi}] = KC \sin(\theta - \xi) \end{aligned}$$

where \Im is the imaginary part of a complex number, i.e. $\Im[a + ib] = b$. The values of $C > 0$ and ξ are calculated using the identity

$$C e^{i\xi} = \int_0^{+\infty} e^{i\psi} g(\psi) d\psi. \tag{25}$$

This complex number, usually called the ‘order parameter’, provides a measure of how the phase lags are distributed within the unit circle. It can also be interpreted as the center of mass of the lags ψ_{ij} ’s when they are thought of as points ($e^{i\psi_{ij}}$) within the unit circle \mathbb{S}^1 . Thus, when $C \approx 1$, the ψ_{ij} ’s are mostly concentrated around ξ . When $C \approx 0$, the delay is distributed such that $\sum_{ij} e^{i\psi_{ij}} \approx 0$. Thus, the equivalent non-delayed system (23) becomes

$$\dot{\phi}_i = \omega + \varepsilon KC \sum_{j \in \mathcal{N}_i} \sin(\phi_j - \phi_i - \xi). \tag{26}$$

In other words, when $N \rightarrow +\infty$ and the natural frequencies are homogeneous, the Kuramoto model with heterogeneous delays behaves as if the delays were homogenous, with $\eta_{ij} = \frac{\xi}{\omega} \forall ij$.

Furthermore, we can see how the distribution of $g(\psi)$ has a direct effect on the dynamics through the parameters C and ξ defined in (25). For example, when the delays are heterogeneous enough such that $C \approx 0$, the coupling term disappears and therefore makes synchronization impossible. A complete study of (26) under the context of superconducting Josephson arrays was performed in [46]. There the authors characterized the condition for in-phase synchronization in terms of K and $C e^{i\xi}$. More precisely, when $K C e^{i\xi}$ is on the right half of the plane ($K C \cos(\xi) > 0$), the system almost always synchronizes. However, when $K C e^{i\xi}$ is on the left half of the plane ($K C \cos(\xi) < 0$), the system moves towards an incoherent state where all of the oscillators’ phases spread around the unit circle such that its order parameter, i.e. $\frac{1}{N} \sum_{l=1}^N e^{i\phi_l}$, becomes zero.

We now provide simulation results to illustrate how (26) becomes a good approximation of the original system when N is large enough. We simulate the original repulsive ($K < 0$) sine-coupled system with heterogeneous delays and its corresponding approximation (26). Two different delay distributions, illustrated in figure 10, were selected such that their corresponding order parameters lie in different half-planes.

The same simulation is repeated for $N = 5, 10, 50$. Figure 11 shows that when N is small, the phases’ order parameter of the original system (in red/blue) draws a trajectory which is completely different with respect to its approximation (in green). However, as N grows, in both cases the trajectories become closer and closer. Since $K < 0$, the trajectory of the system with wider distribution ($C \cos \xi < 0$) drives the order parameter towards the boundary of the circle, i.e., **heterogeneous delay leads to homogeneous phase**.

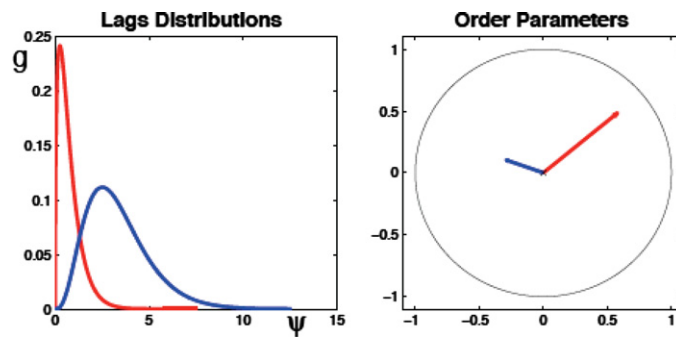


Figure 10. Delay distributions and their order parameter $Ce^{i\xi}$.

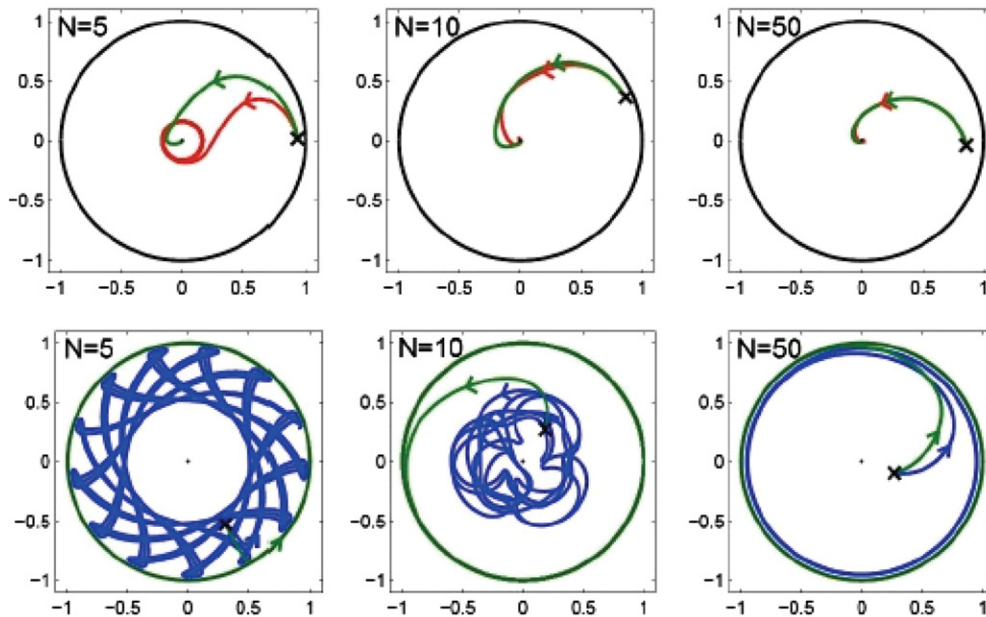


Figure 11. Repulsive sine coupling with heterogeneous delays: the evolution of the order parameter of the system (3) with $K < 0$ (repulsive) and delays drawn from the delay distribution of figure 10 are shown. The colors match the colors of the corresponding distributions. The green trajectory corresponds to the non-delayed approximation (26). As N grows the trajectories become closer.

4.2. Effect of heterogeneity

We now explain a more subtle effect that can be produced by heterogeneity. Consider the system in (23) where H is odd and continuously differentiable. Then, from section 3, all the oscillators eventually end up running at the same speed ω with fixed phase difference such that the sum $\sum_{i \in \mathcal{N}_i} H(\phi_j - \phi_i)$ cancels $\forall i$. Moreover, we can apply (10) to assess the stability of these orbits. Therefore, if we can find a cut C of the network such that $\sum_{ij \in C} H'(\phi_j^* - \phi_i^*) < 0$, the phase-locked solution will be unstable.

Although this condition is for non-delayed phase-coupled oscillators, the result of this section allows us to translate it for systems with delay. Since H is the convolution of the coupling function f and the delay distribution function g , we can obtain $H'(\phi_j^* - \phi_i^*) < 0$, even when $f'(\phi_j^* - \phi_i^*) > 0$. This usually occurs when the convolution widens the region with a negative slope of H . See figure 9 for an illustration of this phenomenon.

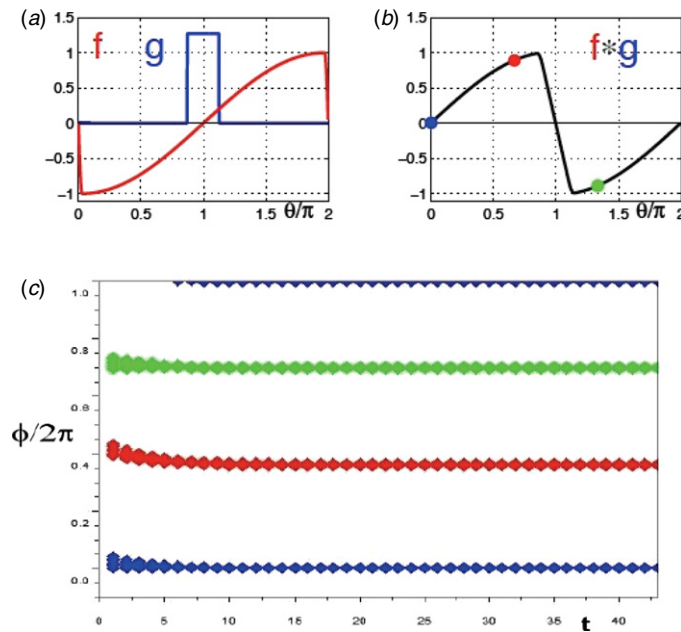


Figure 12. Pulse-coupled oscillators with delay: stable equilibrium; (a) repulsive coupling f and delay distribution g ; (b) corresponding non-delayed approximation H ; (c) oscillators phase snapshot of the system for every time the oscillator number 1 ($i = 1$) fires.

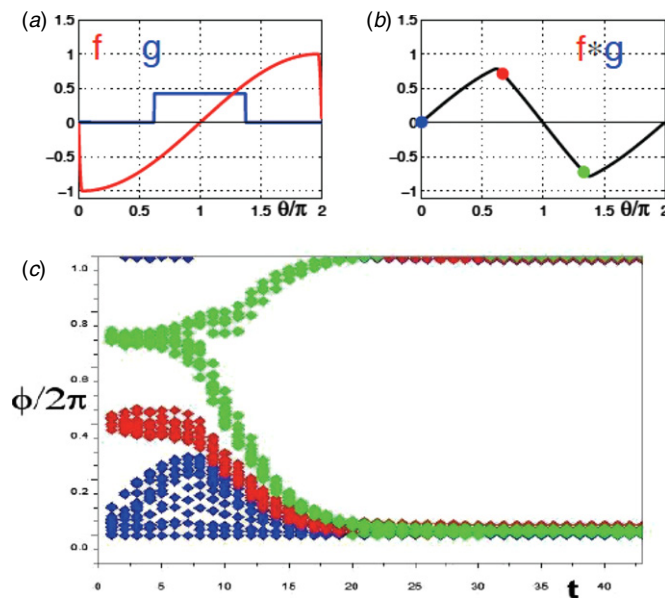


Figure 13. Pulse-coupled oscillators with delay: unstable equilibrium; (a) repulsive coupling f and delay distribution g ; (b) corresponding non-delayed approximation H ; (c) oscillators phase snapshot of the system for every time the oscillator number 1 ($i = 1$) fires.

Figures 12 and 13 show two simulation setups of 45 oscillators **pulse-coupled** all to all. The initial state is close to a phase-locked configuration formed by three equidistant clusters of 15 oscillators each. The shape of the coupling function f and the phase lags distribution g

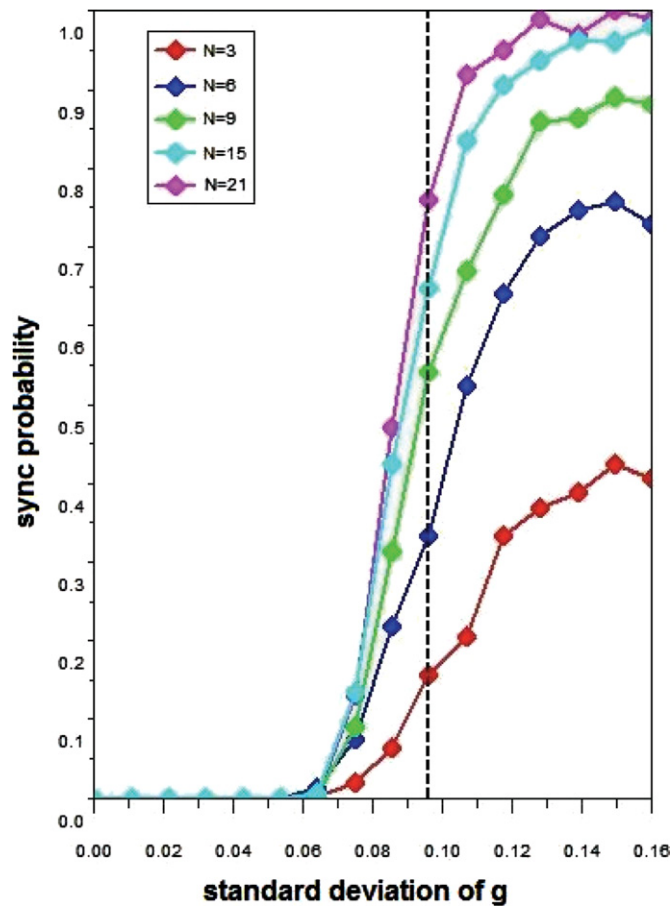


Figure 14. Pulse-coupled oscillators with delay: synchronization probability; each point represent the fraction of times the system with initial condition as in figures 12 and 13 synchronizes in phase for given standard deviation σ and random chosen delays; the dashed line represents the critical σ that makes the non-delayed approximation unstable.

are shown in part a; g is a uniform distribution with mean $\mu = \pi$ and variance σ^2 . We used (4) to implement the corresponding pulse-coupled system (1). While f is maintained unchanged between both simulations, we change the variance, i.e. the heterogeneity, of the distribution g . Thus, the corresponding $H = f * g$ changes as it can be seen in part b; the blue, red and green dots correspond to the speed change induced in an oscillator within the blue cluster by oscillators of each cluster. Since all clusters have the same number of oscillators, the net effect is zero. Part c shows the time evolution of oscillators' phases relative to the phase of a blue cluster oscillator. Although the initial conditions are exactly the same, the wider delay distribution on figure 13 produces negative slope on the red and green points of part b, which destabilizes the clusters and drives oscillators toward in-phase synchrony.

Finally, we simulate the same scenario as in figures 12 and 13 but now changing N and the standard deviation, i.e. the delay distribution width. Figure 14 shows the computation of the synchronization probability versus standard deviation of the uniform distributions of figure. The dashed line denotes the minimum value that destabilizes the equivalent system. As N grows, the distribution shape becomes closer to a step, which is the expected shape in

the limit. It is quite surprising that as soon as the equilibrium is within the region of H with negative slope, the equilibrium becomes unstable as the theory predicts.

5. Conclusion

This paper analyzes the dynamics of identical weakly coupled oscillators while relaxing several classical assumptions on coupling, delay and topology. Our results provide global synchronization guarantees for a wide range of scenarios. There are many directions that can be taken to further this study. For example, for different topologies, to guarantee global in-phase synchronization, how does the requirement on coupling functions change? Another specific question is to complete the proof in section 3.3 for the cases when $m = 1, 3, 5$. Finally, it would be of great interest if we could apply results and techniques in this paper to a wide range of applications such as transient stability analysis of power networks and clock synchronization of computer networks.

Acknowledgments

The authors thank Steven H Strogatz of Cornell for useful discussions.

References

- [1] Winfree A T 1967 Biological rhythms and the behavior of populations of coupled oscillators *J. Theor. Biol.* **16** 15–42
- [2] Peskin C S 1975 *Mathematical Aspects of Heart Physiology* (New York: Courant Institute of Mathematical Science)
- [3] Achermann P and Kunz H 1999 Modeling circadian rhythm generation in the suprachiasmatic nucleus with locally coupled self-sustained oscillators: phase shifts and phase response curves *J. Biol. Rhythms* **14** 460–8
- [4] Garcia-Ojalvo J, Elowitz M B, Strogatz S H and Peskin C S 2004 Modeling a synthetic multicellular clock: repressilators coupled by quorum sensing *Proc. Natl Acad. Sci. USA* **101** 10955–60
- [5] Yamaguchi S, Isejima H, Matsuo T, Okura R, Yagita K, Kobayashi M and Okamura H 2003 Synchronization of cellular clocks in the suprachiasmatic nucleus *Science* **32** 1408–12
- [6] Kiss I Z, Zhai Y and Hudson J L 2002 Emerging coherence in a population of chemical oscillators *Science* **296** 1676–8
- [7] York R A and Compton R C 1991 Quasi-optical power combining using mutually synchronized oscillator arrays *IEEE Trans. Microw. Theory Tech.* **39** 1000–9
- [8] Hong Y-W and Scaglione A 2005 A scalable synchronization protocol for large scale sensor networks and its applications *IEEE J. Sel. Areas Commun.* **23** 1085–99
- [9] Werner-Allen G, Tewari G, Patel A, Welsh M and Nagpal R 2005 Firefly-inspired sensor network synchronicity with realistic radio effects *SensSys: Proc. of the 3rd Int. Conf. on Embedded Networked Sensor Systems* (New York: ACM) pp 142–53
- [10] Marvel S A and Strogatz S H 2009 Invariant submanifold for series arrays of Josephson junctions *Chaos* **19** 013132
- [11] Bressloff P C and Coombes S 1999 Travelling waves in chains of pulse-coupled integrate-and-fire oscillators with distributed delays *Physica D* **130** 232–54
- [12] Ashwin P and Swift J W 1992 The dynamics of n weakly coupled identical oscillators *J. Nonlinear Sci.* **2** 69–108
- [13] Ermentrout G B 1992 Stable periodic solutions to discrete and continuum arrays of weakly coupled nonlinear oscillators *SIAM J. Appl. Math.* **52** 1665–87
- [14] Kuramoto Y 1975 *International Symposium on Mathematical Problems in Theoretical Physics (Lecture Notes in Physics vol 39)* ed H Arakai (New York: Springer) p 420
- [15] Popovych O V, Maistrenko Y L and Tass P A 2005 Phase chaos in coupled oscillators *Phys. Rev. E* **71** 065201
- [16] Brown E, Holmes P and Moehlis J 2003 Globally coupled oscillator networks *Perspectives and Problems in Nonlinear Science: A Celebratory Volume in Honor of Larry Sirovich* (New York: Springer) pp 183–215
- [17] Jadbabaie A, Moten N and Barahona M 2004 On the stability of the Kuramoto model of coupled nonlinear oscillators *Proc. American Control Conf. (Boston, 30 June)* vol 5 pp 4296–301

- [18] Lucarelli D and Wang I-J 2004 Decentralized synchronization protocols with nearest neighbor communication *Proc. 2nd Int. Conf. on Embedded Networked Sensor Systems* pp 62–8
- [19] Monzón P and Paganini F 2005 Global considerations on the Kuramoto model of sinusoidally coupled oscillators *Proc. 44th IEEE Conf. on Decision and Control, and European Control Conf. (Sevilla, Spain, December 1985)* pp 3923–8
- [20] Mirollo R E and Strogatz S H 1990 Synchronization of pulse-coupled biological oscillators *SIAM J. Appl. Math.* **50** 1645–62
- [21] Moreau L 2004 Stability of continuous-time distributed consensus algorithms *43rd IEEE Conf. on Decision and Control* vol 4 pp 3998–4003
- [22] Ren W and Beard R W 2004 Consensus of information under dynamically changing interaction topologies *Proc. 2004 American Control Conf. (30 June–2 July)* vol 6 pp 4939–44
- [23] Stan G-B and Sepulchre R 2003 Dissipativity characterization of a class of oscillators and networks of oscillators *Proc. 42nd IEEE Conf. on Decision and Control (December)* vol 4 pp 4169–73
- [24] Scardovi L, Sarlette A and Sepulchre R 2007 Synchronization and balancing on the n-torus *Syst. Control Lett.* **56** 335–41
- [25] Sepulchre R, Paley D A and Leonard N E 2008 Stabilization of planar collective motion with limited communication *IEEE Trans. Autom. Control* **53** 706–19
- [26] Papachristodoulou A and Jadbabaie A 2006 Synchronization in oscillator networks with heterogeneous delays, switching topologies and nonlinear dynamics *Proc. 45th IEEE Conf. on Decision and Control* pp 4307–12
- [27] Izhikevich E M 1998 Phase models with explicit time delays *Phys. Rev. E* **58** 905–8
- [28] Izhikevich E M 1999 Weakly pulse-coupled oscillators, fm interactions, synchronization, and oscillatory associative memory *IEEE Trans. Neural Netw.* **10** 508–26
- [29] Mallada E and Tang A 2010 Synchronization of phase-coupled oscillators with arbitrary topology *Proc. American Control Conf.* pp 1777–82
- [30] Mallada E and Tang A 2010 Weakly pulse-coupled oscillators: heterogeneous delays lead to homogeneous phase *Proc. 49th IEEE Conf. on Decision and Control* pp 992–7
- [31] Ernst U, Pawelzik K and Geisel T 1995 Synchronization induced by temporal delays in pulse-coupled oscillators *Phys. Rev. Lett.* **74** 1570–3
- [32] Ernst U, Pawelzik K and Geisel T 1998 Delay-induced multistable synchronization of biological oscillators *Phys. Rev. E* **57** 2150–62
- [33] Kuramoto Y 1984 *Chemical Oscillations, Waves, and Turbulence* (Berlin: Springer)
- [34] Sepulchre R, Paley D A and Leonard N E 2007 Stabilization of planar collective motion: all-to-all communication *IEEE Trans. Autom. Control* **52** 811–24
- [35] Daido H 1992 Quasientrainment and slow relaxation in a population of oscillators with random and frustrated interactions *Phys. Rev. Lett.* **68** 1073–6
- [36] Rantzer A 2001 A dual to Lyapunov’s stability theorem *Syst. Control Lett.* **42** 161–8
- [37] Bollobas B 1998 *Modern Graph Theory* (New York: Springer)
- [38] Godsil C and Royle G 2001 *Algebraic Graph Theory* (New York: Springer)
- [39] Khalil H K 1996 *Nonlinear Systems* 3rd edn (Englewood Cliffs, NJ: Prentice-Hall)
- [40] Hoppensteadt F C and Izhikevich E M 1997 *Weakly Connected Neural Networks* (New York: Springer)
- [41] Sarlette A 2009 Geometry and symmetries in coordination control *PhD Thesis* University of Liège, Belgium
- [42] van Vreeswijk C, Abbott L and Ermentrout G B 1994 When inhibition not excitation synchronizes neural firing *J. Comput. Neurosci.* **1** 313–21
- [43] Gerstner W 1996 Rapid phase locking in systems of pulse-coupled oscillators with delays *Phys. Rev. Lett.* **76** 1755–8
- [44] Aonishi T and Okada M 2002 Dynamically-coupled oscillators—cooperative behavior via dynamical interaction arXiv:condmat/0207506
- [45] Lee W S, Ott E and Antonsen T M 2009 Large coupled oscillator systems with heterogeneous interaction delays *Phys. Rev. Lett.* **103** 044101
- [46] Watanabe S and Strogatz S H 1994 Constants of motion for superconducting Josephson arrays *Physica D* **74** 197–253
- [47] Sakaguchi H and Kuramoto Y 1986 A soluble active rotator model showing phase transitions via mutual entertainment *Prog. Theor. Phys.* **76** 576–81
- [48] Yeung M K S and Strogatz S H 1999 Time delay in the kuramoto model of coupled oscillators *Phys. Rev. Lett.* **82** 648